

SOC-MARTNET: A MARTINGALE NEURAL NETWORK FOR THE HAMILTON-JACOBI-BELLMAN EQUATION WITHOUT EXPLICIT $\inf_{U \in U} H$ IN STOCHASTIC OPTIMAL CONTROLS *

WEI CAI[†], SHUOXIN FANG[‡], AND TAO ZHOU[§]

Abstract. In this paper, we propose a martingale-based neural network, SOC-MartNet, for solving high-dimensional Hamilton-Jacobi-Bellman (HJB) equations where no explicit expression is needed for the infimum of the Hamiltonian, $\inf_{u \in U} H(t, x, u, z, p)$, and stochastic optimal control problems (SOCs) with controls on both drift and volatility. We reformulate the HJB equations for the value function by training two neural networks, one for the value function and one for the optimal control with the help of two stochastic processes - a Hamiltonian process and a cost process. The control and value networks are trained such that the associated Hamiltonian process is minimized to satisfy the minimum principle of a feedback SOCP, and the cost process becomes a martingale, thus, ensuring the value function network as the solution to the corresponding HJB equation. Moreover, to enforce the martingale property for the cost process, we employ an adversarial network and construct a loss function characterizing the projection property of the conditional expectation condition of the martingale. Numerical results show that the proposed SOC-MartNet is effective and efficient for solving HJB-type equations and SOCPs with a dimension up to 10,000 in a small number of iteration steps (less than 6000) of training.

Key words. Hamilton-Jacobi-Bellman equation; high dimensional PDE; stochastic optimal control; deep neural networks; adversarial networks; martingale formulation.

MSC codes. 49L12, 49L20, 49M05, 65C30, 93E20

1. Introduction. In this paper, we consider the numerical solution of high-dimensional Hamilton-Jacobi-Bellman (HJB)-type equations and their applications to stochastic optimal control problems (SOCs). The considered HJB-type equation is given in the form of

$$(1.1) \quad \partial_t v(t, x) + \mathcal{L}v(t, x) + \inf_{\kappa \in U} H(t, x, \kappa, \partial_x v(t, x), \partial_{xx}^2 v(t, x)) = 0$$

for $(t, x) \in [0, T] \times \mathbb{R}^d$ with $\partial_x = \nabla_x$ and $\partial_{xx}^2 = \nabla_x \nabla_x^\top$ as the gradient and Hessian operator, respectively, and a terminal condition

$$(1.2) \quad v(T, x) = g(x), \quad x \in \mathbb{R}^d,$$

where \mathcal{L} is a differential operator given by

$$(1.3) \quad \mathcal{L} := \mu^\top(t, x) \partial_x + \frac{1}{2} \text{Tr} \{ \sigma \sigma^\top(t, x) \partial_{xx}^2 \}$$

for some given functions $\mu : [0, T] \times \mathbb{R}^d \rightarrow \mathbb{R}^d$ and $\sigma : [0, T] \times \mathbb{R}^d \rightarrow \mathbb{R}^{d \times q}$; $H(t, x, \kappa, z, p)$ is the Hamiltonian as a mapping $(t, x, \kappa, z, p) \in [0, T] \times \mathbb{R}^d \times U \times \mathbb{R}^d \times \mathbb{R}^{d \times d} \rightarrow \mathbb{R}$, and

*This work of SF and TZ is supported by the NSF of China (under grant 12288201) and the Youth Innovation Promotion Association (CAS). Date. July 8, 2024. *Previous version of this manuscript is published on arxiv arXiv:2405.03169, May 6, 2024*

[†]Department of Mathematics, Southern Methodist University, Dallas, TX 75275, USA. Corresponding author. (cai@smu.edu).

[‡]Institute of Computational Mathematics and Scientific/Engineering Computing, Academy of Mathematics and Systems Science, Chinese Academy of Sciences, Beijing, 100190, P. R. China. (sxfang@amss.ac.cn).

[§]Institute of Computational Mathematics and Scientific/Engineering Computing, Academy of Mathematics and Systems Science, Chinese Academy of Sciences, Beijing, 100190, P. R. China. Corresponding author. (tzhoul@lsec.cc.ac.cn).

$U \subset \mathbb{R}^m$. The HJB-type equation (1.1) is general and covers common HJB equations in SOCPs; see the discussions in section 3. In addition to this equation, this paper also explores the application of the proposed method to common semi-linear parabolic equations without boundary conditions.

The HJB equation is a fundamental partial differential equation (PDE) in the field of optimal control theory [7, 14, 37, 42, 49]. In the typical framework of dynamic programming [3, 14], the optimal feedback control is identified by the verification technique, which involves minimizing a Hamiltonian depending on the derivatives of a value function [49, p. 278]. On this account, the HJB equation, which governs this value function, stands as a cornerstone of dynamic programming. The well-posedness of HJB equations has been firmly established with the theory of viscosity solutions; see, e.g., [8, 27, 39]. But solving the HJB equation is still challenging due to its non-smoothness and high dimensionality.

The wide application of HJB equations has spurred extensive research on efficient numerical methods. Conventional approaches include the Galerkin method [47], the finite volume method [41, 45], the monotone approximation scheme [2], the patchy dynamic programming [4], etc. These methods generally suffer from the curse of dimensionality (CoD) [3], that is, the computation complexity increases exponentially with the dimension of the HJB equations. In [31, 32], the HJB equation is solved through the associated BSDE deduced from a Feynman-Kac representation [33], but the resolution of BSDE relies on least square regression on a set of basis functions, where the CoD arises since the number of required basis functions explodes with the dimension. There are also literature leveraging dimension reduction techniques, e.g., [12, 29, 30], but these techniques depend on the dimension reducibility of the problem.

In recent years, deep learning has emerged as a promising tool to overcome the CoD, leading to a growing body of deep learning methods for solving high dimensional PDEs, e.g., [13, 16, 19, 21, 24, 26, 44, 50, 51]. While demonstrably effective for usual high-dimensional PDEs, these methods encounter new challenges when applied to the HJB-type equation (1.1). One of the challenges stems from the inherent infimum operator $\inf_{\kappa \in U}$ imposed on the Hamiltonian H in the HJB equation. Directly minimizing the Hamiltonian for every time-space point (t, x) is computationally expensive, in fact, a CoD problem itself for high dimensional control spaces.

To avoid this issue, the works in [9–11, 24] focus on Hamilton-Jacobi equations where $\inf_{\kappa \in U} H$ is explicitly known. The work [40, section 3.4] considers specific optimal control problems such that $\inf_{\kappa \in U} H$ admits an analytic expression. There are also research resorting to deep neural networks (DNNs). For example, [28, section 3.2] introduces a DNN to learn the feedback control $u(t, x)$ such that $u(t, x)$ becomes a stationary point of H , i.e., $\partial_{\kappa} H|_{\kappa=u(t,x)} = 0$, whereas certain conditions on U and H are needed to ensure the stationary point is a minimizer of $\kappa \mapsto H$. The paper [53] considers static HJB-type PDEs, where solving $\inf_{\kappa \in U} H$ is avoided by reformulating the problem into a SOCP solved by reinforcement learning. In [38], the authors propose a neural network approach for high-dimensional SOCPs, using the stochastic Pontryagin maximum principle to guide a forward SDE for state-space exploration for handling problems with complex dynamics. In addition, there are works on numerical methods for SOCPs by not explicitly solving the HJB equation, e.g., [1, 15, 18, 20, 25, 52]. At this time, developing new efficient numerical methods for high-dimensional HJB equations still remains an actively researched topic.

In this paper, we propose a new approach for solving the high-dimensional HJB-type equation (1.1). In our approach, the control and value functions of the prob-

lem are approximated by DNNs. The HJB equation is encoded into a Hamiltonian process and a cost process both depending on the control network and the value network. The value and the control networks are trained by minimizing a functional of the Hamiltonian process while ensuring the cost process to be a martingale, which guarantees the value function is the solution to the HJB equation. The martingale property is enforced by an adversarial learning, whose loss function is constructed by characterizing the projection property of conditional expectations. The proposed method, named SOC-MartNet, is able to solve high dimensional stochastic optimal control problems, by using the the approach of a martingale formulation, originally developed in the DeepMartNet for boundary value and eigenvalue problems of high dimensional PDEs [5, 6]. Our numerical experiments show that the proposed SOC-MartNet is highly effective and efficient for solving equations with dimension up to 2000 in a small number of iterations of training.

In the SOC-MartNet method, the task of finding $\inf_{\kappa \in U} H$ for each (t, x) is accomplished by training an optimal control network to minimize a functional of the Hamiltonian process, and avoiding the need of evaluating explicitly the infimum in the HJB equation. Moreover, the training algorithm enjoys parallel efficiency as it is free of time-directed iterations during gradient computation. This feature is much different from existing deep-learning probabilistic methods for PDEs. The SOC-MartNet also demonstrates broad applicability, effectively handling high-dimensional HJB equations and parabolic equations as well as SOCPs.

The remainder of this paper is organized as follows. In section 2, we briefly review the main ideas in dynamic programming and minimum principle for solving SOCPs as well as the proposed computational approach. In section 3, we propose the SOC-MartNet and its algorithm for general non-degenerated HJB equations and parabolic equations. Numerical results are presented in section 4. A conclusion and plan for future work are given in section 5.

2. Dynamic programming and minimum principle, and computational approach. We consider a filtered complete probability space $(\Omega, \mathcal{F}, \mathbb{F}^B, \mathbb{P})$ with $\mathbb{F}^B := (\mathcal{F}_t)_{0 \leq t \leq T}$ as the natural filtration of the standard q -dimensional Brownian motion $B = (B_t)_{0 \leq t \leq T}$, and $T \in (0, \infty)$ a deterministic terminal time. Let \mathcal{U}_{ad} be the set of admissible feedback control functions defined by

$$(2.1) \quad \mathcal{U}_{\text{ad}} := \{u : [0, T] \times \mathbb{R}^d \rightarrow U \mid u \text{ is Borel measurable}\} \quad \text{with } U \subset \mathbb{R}^m.$$

For any $u \in \mathcal{U}_{\text{ad}}$, the controlled state process X^u is governed by the following stochastic differential equation (SDE):

$$(2.2) \quad X_t^u = x_0 + \int_0^t \bar{\mu}(s, X_s^u, u(s, X_s^u)) ds + \int_0^t \bar{\sigma}(s, X_s^u, u(s, X_s^u)) dB_s, \quad t \in [0, T]$$

with $x_0 \in \mathbb{R}^d$, where $\bar{\mu} : [0, T] \times \mathbb{R}^d \times U \rightarrow \mathbb{R}^d$ and $\bar{\sigma} : [0, T] \times \mathbb{R}^d \times U \rightarrow \mathbb{R}^d$ are the controlled drift coefficient and controlled diffusion coefficient, respectively, and the stochastic integral with respect to B_s is of Itô type. The cost functional of u is given by

$$(2.3) \quad J(u) := \mathbb{E} \left[\int_0^T c(s, X_s^u, u(s, X_s^u)) ds + g(X_T^u) \right],$$

where $c : [0, T] \times \mathbb{R}^d \times U \rightarrow \mathbb{R}$ and $g : \mathbb{R}^d \rightarrow \mathbb{R}$ characterize the running cost and terminal cost, respectively. Our main focus is the following SOCP:

$$(2.4) \quad \text{Find } u^* \in \mathcal{U}_{\text{ad}} \text{ such that } J(u^*) = \inf_{u \in \mathcal{U}_{\text{ad}}} J(u).$$

To carry out the approach of dynamic programming, we define the value function v by $v(t, x) := \inf_{u \in \mathcal{U}_{\text{ad}}} J(t, x, u)$ with

$$J(t, x, u) := \mathbb{E} \left[\int_t^T c(s, X_s^u, u(s, X_s^u)) \, ds + g(X_T^u) \middle| X_t^u = x \right]$$

for $(t, x) \in [0, T] \times \mathbb{R}^d$. Under certain conditions (see, e.g., [42, Theorem 4.3.1 and Remark 4.3.4]), the value function v is the viscosity solution to the following fully nonlinear HJB equation

$$(2.5) \quad \partial_t v(t, x) + \inf_{\kappa \in U} H(t, x, \kappa, \partial_x v(t, x), \partial_{xx}^2 v(t, x)) = 0, \quad (t, x) \in [0, T] \times \mathbb{R}^d$$

with the terminal condition $v(T, x) = g(x)$, $x \in \mathbb{R}^d$, and the Hamiltonian H given by

$$(2.6) \quad H(t, x, \kappa, z, p) := \frac{1}{2} \text{Tr}(p \bar{\sigma} \sigma^\top(t, x, \kappa)) + z^\top \bar{\mu}(t, x, \kappa) + c(t, x, \kappa)$$

for $(t, x, \kappa, z, p) \in [0, T] \times \mathbb{R}^d \times U \times \mathbb{R}^d \times \mathbb{R}^{d \times d}$.

Under the regularity condition $v \in C^{1,2}$, i.e., v is once and twice continuously differentiable with respect to $t \in [0, T]$ and $x \in \mathbb{R}^d$, respectively, the classical verification theorem (see, e.g., [7] or [49, p. 268, Theorem 5.1]) reveals the optimal feedback control as

$$(2.7) \quad u^*(t, X_t^*) \in \arg \min_{\kappa \in U} H(t, X_t^*, \kappa, \partial_x v(t, X_t^*), \partial_{xx}^2 v(t, X_t^*)), \quad t \in [0, T],$$

where $X^* := X^{u^*}$ is the controlled diffusion defined in (2.2) corresponding to the optimal control u^* . The above equation (2.7) implies that for $t \in [0, T]$

$$(2.8) \quad \begin{aligned} & H(t, X_t^*, u^*(t, X_t^*), \partial_x v(t, X_t^*), \partial_{xx}^2 v(t, X_t^*)) \\ &= \inf_{\kappa \in U} H(t, X_t^*, \kappa, \partial_x v(t, X_t^*), \partial_{xx}^2 v(t, X_t^*)). \end{aligned}$$

Therefore, by the minimum principle (2.8), to find the optimal feedback control, it is sufficient to ensure

$$(2.9) \quad u^*(t, x) \in \arg \min_{\kappa \in U} H(t, x, \kappa, \partial_x v(t, x), \partial_{xx}^2 v(t, x)), \quad x \in \Gamma_t, \quad t \in [0, T],$$

or for all $t \in [0, T]$ and $x \in \Gamma_t$,

$$(2.10) \quad \begin{aligned} & H(t, x, u^*(t, x), \partial_x v(t, x), \partial_{xx}^2 v(t, x)) \\ &= \inf_{\kappa \in U} H(t, x, \kappa, \partial_x v(t, x), \partial_{xx}^2 v(t, x)) \end{aligned}$$

for some state set $\Gamma_t \supset \Gamma(X_t^*)$, where $\Gamma(X_t^*)$ denotes the support set of the probability density function of X_t^* .

Computational approach. On the basis of (2.10), the key step for solving the SOCP (2.4) is then to find the value function v from the HJB equation (2.5), but, the

evaluation of the $\inf_{\kappa \in U} H$ in the the HJB equation (2.4), thus finding $v(t, x)$, suffers from the CoD for a high dimensional control space. However, if the optimal control u^* is known, then from the minimum principle (2.10), the HJB equation is reduced to, without the inf operation,

$$(2.11) \quad \partial_t v(t, x) + H(t, x, u^*(t, x), \partial_x v(t, x), \partial_{xx}^2 v(t, x)) = 0, \quad (t, x) \in [0, T] \times \Gamma_t.$$

This argument suggests that we should consider a computational approach, which produces approximations simultaneously to both the value function v and the optimal control u^* represented by separate neural networks, to ensure that (2.11) will hold once the training of the networks leads to convergence. Therefore, before the convergence of the network for the optimal control, the value network is in fact an approximation to a version of the HJB equation (2.11) where the optimal control u^* is replaced with its neural network approximation. Similarly, the infimum of the Hamiltonian in (2.10) is taken with the value function replaced by its network approximation. It is expected that once both networks have converged, the correct forms of HJB equation and the infimum of Hamiltonian will have been enforced to yield both the optimal control and value function. This will be the approach of the proposed numerical method.

3. Proposed method. Throughout this section, we assume that the HJB-type equation (1.1) admits a classical solution $v \in C^{1,2}$, where the regularity of v is needed for the martingale formulation. According to standard PDE theory (see, e.g., [36, Section 6.2, Theorem 5]), this regularity follows from the non-degeneracy condition of (1.1), i.e., $\sigma \sigma^\top(t, x)$ in (1.3) is uniformly positive definite on $[0, T] \times \mathbb{R}^d$. Below, we show that (1.1) covers many useful cases, including:

- **SOC (2.4) without volatility control.** If $\bar{\sigma}(t, x, \kappa) = \bar{\sigma}(t, x)$, the HJB equation (2.5) degenerates into a special case of (1.1) with

$$\mathcal{L} = \frac{1}{2} \text{Tr} \{ \bar{\sigma} \bar{\sigma}^\top(t, x) \partial_{xx}^2 \}, \quad H(t, x, \kappa, z, p) = z^\top \bar{\mu}(t, x, \kappa) + c(t, x, \kappa)$$

for $(t, x, \kappa, z, p) \in [0, T] \times \mathbb{R}^d \times U \times \mathbb{R}^d \times \mathbb{R}^{d \times d}$.

- **Controlled volatility $\bar{\sigma}$ with an uncontrolled part.** If the $\bar{\sigma}$ admits a decomposition as $\bar{\sigma}(t, x, \kappa) = \bar{\sigma}_0(t, x) + \bar{\sigma}_1(t, x, \kappa)$ for some $\mathbb{R}^{d \times q}$ -valued functions $\bar{\sigma}_0$ and $\bar{\sigma}_1$, then the HJB equation (2.5) becomes a special case of (1.1) with

$$\begin{aligned} \mathcal{L} &= \frac{1}{2} \text{Tr} \{ \bar{\sigma}_0 \bar{\sigma}_0^\top(t, x) \partial_{xx}^2 \}, \\ H(t, x, \kappa, z, p) &= \frac{1}{2} \text{Tr} [p \Sigma(t, x, \kappa)] + z^\top \bar{\mu}(t, x, \kappa) + c(t, x, \kappa), \\ \Sigma(t, x, \kappa) &:= \bar{\sigma}_0(t, x) \bar{\sigma}_0^\top(t, x, \kappa) + \bar{\sigma}_1(t, x, \kappa) \bar{\sigma}_0^\top(t, x) + \bar{\sigma}_1(t, x, \kappa) \bar{\sigma}_1^\top(t, x, \kappa) \end{aligned}$$

for $(t, x, \kappa, z, p) \in [0, T] \times \mathbb{R}^d \times U \times \mathbb{R}^d \times \mathbb{R}^{d \times d}$.

- **Knowledge of some preliminary approximation u_0 for the optimal control u^* .** In this case, the HJB equation (2.5) can be rewritten into (1.1) with

$$\mathcal{L} = \mathcal{L}^{u_0}, \quad H(t, x, \kappa, \partial_x v(t, x), \partial_{xx}^2 v(t, x)) = (\mathcal{L}^\kappa - \mathcal{L}^{u_0}) v(t, x) + c(t, x, \kappa),$$

where

$$\mathcal{L}^\kappa := \bar{\mu}^\top(t, x, \kappa) \partial_x + \frac{1}{2} \text{Tr} \{ \bar{\sigma} \bar{\sigma}^\top(t, x, \kappa) \partial_{xx}^2 \} \quad \text{for } \kappa \in U$$

with the convention $\mathcal{L}^u v(t, x) := \mathcal{L}^{u(t, x)} v(t, x)$.

- **Explicit form of the optimal control in the Hamiltonian.** If the following function \bar{H} is explicitly known:

$$\bar{H}(t, x, z, p) := \inf_{u \in U} H(t, x, u, z, p), \quad (t, x, z, p) \in [0, T] \times \mathbb{R}^d \times \mathbb{R}^{d \times d},$$

then (1.1) degenerates into a parabolic equation as

$$(3.1) \quad \partial_t v(t, x) + \mathcal{L}v(t, x) + \bar{H}(t, x, \partial_x v(t, x), \partial_{xx}^2 v(t, x)) = 0.$$

From the above discussions, the SOC-MartNet designed for the HJB-type equation (1.1) is applicable for the SOCP (2.4) with non-degenerated diffusion and the parabolic equation (3.1) without boundary conditions.

3.1. Martingale formulation for HJB-type equations. Let $X : [0, T] \times \Omega \rightarrow \mathbb{R}^d$ be a uncontrolled diffusion process associated with the operator \mathcal{L} , i.e.,

$$(3.2) \quad X_t = X_0 + \int_0^t \mu(s, X_s) ds + \int_0^t \sigma(s, X_s) dB_s, \quad t \in [0, T].$$

Hamiltonian process $H_t^{u,v}$ and cost process $\mathcal{M}_t^{u,v}$ for $t \in [0, T]$. Using the optimal control $u \in \mathcal{U}_{\text{ad}}$ and the value function v , we define two processes - a Hamiltonian process $H_t^{u,v}$, which will be used for enforcing the minimum principle (2.10),

$$(3.3) \quad H_t^{u,v} = H^{u,v}(t, X_t) := H(t, X_t, u(t, X_t), \partial_x v(t, X_t), \partial_{xx}^2 v(t, X_t)),$$

and, a cost process $\mathcal{M}_t^{u,v}$, whose being a martingale implies that the value function $v(t, x)$ satisfies the HJB equation (2.11),

$$(3.4) \quad \mathcal{M}_t^{u,v} = \mathcal{M}^{u,v}(t, X_t) := v(t, X_t) + \int_0^t H_s^{u,v} ds.$$

Specifically, we aim at finding a set of sufficient conditions on $\mathcal{M}^{u,v}$ and $H^{u,v}$, under which v satisfies the HJB-type equation (1.1), and u is the optimal feedback control in sense of (2.10), as mentioned in the comment after (2.11).

Recalling (2.10), we assume that the uncontrolled diffusion X_t can explore the whole support set of X_t^* (see Remark 3.1), i.e.,

$$(3.5) \quad \Gamma_t = \Gamma(X_t) \supset \Gamma(X_t^*), \quad t \in [0, T].$$

Then, to establish (2.10), it is sufficient to consider the condition

$$(3.6) \quad H_t^{u,v} = H^{u,v}(t, X_t) = \inf_{\kappa \in U} H(t, X_t, \kappa, \partial_x v(t, X_t), \partial_{xx}^2 v(t, X_t)), \quad t \in [0, T].$$

Remark 3.1. (State spaces of controlled and uncontrolled diffusion) For the SOCP (2.4), we introduce the following two strategies to meet the inclusion condition (3.5):

- We randomly take the starting point X_0 of the uncontrolled diffusion X such that the distribution of X_0 covers a neighborhood of $X_0^* = x_0$ in (2.2), e.g., $X_0 \sim N(x_0, rI_d)$ with $r > 0$ a hyper parameter.

- The uncontrolled diffusion can be taken as X^{u_0} given by (2.2) with u_0 as an initial approximation of u^* . Then, we turn to solve the following equation equivalent to (2.5):

$$(\partial_t + \mathcal{L}^{u_0}) v(t, x) + \inf_{\kappa \in U} \{(\mathcal{L}^\kappa - \mathcal{L}^{u_0})v(t, x) + c(t, x, \kappa)\} = 0$$

for $(t, x) \in [0, T] \times \mathbb{R}^d$, for which the Hamiltonian process in (3.3) is given by

$$H_t^{u,v} = (\mathcal{L}^u - \mathcal{L}^{u_0}) v(t, X_t^{u_0}) + c(t, X_t^{u_0}, u(t, X_t^{u_0})), \quad t \in [0, T].$$

The condition (3.6) will be enforced as part of the training for the value and control neural network, but, in order to avoid point-wise application of this condition in a time-space (t, x) region, which is a source of CoD issue, we will reformulate the condition into an integral form in the following lemma, which can be sampled in the fashion of a Monte Carlo method for an empirical loss function.

LEMMA 3.2. *Let v be any Borel measurable function from $[0, T] \times \mathbb{R}^d$ to \mathbb{R} such that*

$$(3.7) \quad \int_0^T \mathbb{E} \left[\left| \inf_{\kappa \in U} H(t, X_t, \kappa, \partial_x v(t, X_t), \partial_{xx}^2 v(t, X_t)) \right| \right] dt < \infty.$$

Assume the optimal feedback control exists under v , i.e., the following equation (3.8) admits a solution $u \in \mathcal{U}_{\text{ad}}$:

$$(3.8) \quad H_t^{u,v} = \inf_{\kappa \in U} H(t, X_t, \kappa, \partial_x v(t, X_t), \partial_{xx}^2 v(t, X_t))$$

for $(t, \omega) \in [0, T] \times \Omega$, a.e.- $dt \times \mathbb{P}$. Then, an optimal control u for (3.8) can be found from the following minimization problem: finding a $u \in \mathcal{U}_{\text{ad}}$ such that

$$(3.9) \quad \int_0^T \mathbb{E} [H_t^{u,v}] dt = \inf_{\bar{u} \in \mathcal{U}_{\text{ad}}} \int_0^T \mathbb{E} [H_t^{\bar{u},v}] dt.$$

Proof. The existence of solution u for the minimization problem (3.9) is evident by taking $\int_0^T \mathbb{E} [\cdot] dt$ on both sides of (3.8).

Next, recalling the definition in (3.6), we assume that there is a $\bar{u} \in \mathcal{U}_{\text{ad}}$ as an optimal feedback control satisfying (3.8), i.e.,

$$(3.10) \quad H_t^{\bar{u},v} = \inf_{\kappa \in U} H(t, X_t, \kappa, \partial_x v(t, X_t), \partial_{xx}^2 v(t, X_t))$$

for $(t, \omega) \in [0, T] \times \Omega$, a.e.- $dt \times \mathbb{P}$. Then, if $u \in \mathcal{U}_{\text{ad}}$ satisfying (3.9), then by its definition, we have that $\int_0^T \mathbb{E} [H_t^{u,v}] dt \leq \int_0^T \mathbb{E} [H_t^{\bar{u},v}] dt$. Inserting (3.10) into the right-side of this inequality, and further using (3.7), we obtain

$$\int_0^T \mathbb{E} [\varepsilon_t] dt \leq 0,$$

where

$$\varepsilon_t = \varepsilon(t, X_t) := H_t^{u,v} - \inf_{\kappa \in U} H(t, X_t, \kappa, \partial_x v(t, X_t), \partial_{xx}^2 v(t, X_t)).$$

On the other hand, the definition of $\varepsilon(t, X_t)$ implies that ε_t is a nonnegative function of (t, X_t) , namely, $\varepsilon_t \geq 0$ for any $t \in [0, T]$. Thus it follows from [34, Theorem 4.8 (i)] that

$$\varepsilon_t = 0 \text{ for } (t, \omega) \in [0, T] \times \Omega, \text{ a.e.-dt} \times \mathbb{P},$$

which implies an optimal control u for (3.8). \square

Remark 3.3. (Integral form of minimum principle and avoiding the CoD problem in (t, x) variables) Lemma 3.2 allows us to replace the minimum principle in (3.8) in a point-wise (t, X_t) sense by an integral version of the minimum principle defined in (3.9). The latter offers significant computational benefits, as the minimization is for a functional (defined by a double integral) on the admissible control set \mathcal{U}_{ad} only, instead of the Hamiltonian on the control space U for each possible time-state (t, X_t) . More importantly, the high dimensional double integral in (t, x) can be carried out in the space-time domain in a Monte Carlo fashion, thus avoiding the CoD problem from the high dimension of X_t and allowing independent sampling of t and x variables for an efficient parallel implementation.

Utilizing the condition (3.8), we can simplify the HJB-type equation (1.1) into

$$(3.11) \quad (\partial_t + \mathcal{L})v(t, X_t) = -H_t^{u,v}(t, X_t)$$

for $t \in [0, T]$. Next, we will show that (3.11) can be fulfilled by enforcing the cost process $\mathcal{M}^{u,v}$ in (3.4) to be a martingale with the value function v and the optimal control u . The following lemma presents the details.

LEMMA 3.4. *For any $(u, v) \in \mathcal{U}_{\text{ad}} \times C^{1,2}$ satisfying*

$$(3.12) \quad \int_0^T \mathbb{E} [|\partial_x v \sigma(t, X_t)|^2] dt < \infty, \quad \int_0^T \mathbb{E} [H_t^{u,v}] dt < \infty, \quad \mathbb{E} [v(T, X_T)] < \infty,$$

the equation (3.11) holds for $(t, \omega) \in [0, T] \times \Omega$ a.e.-dt $\times \mathbb{P}$ if and only if $M_t^{u,v}(t, X_t)$ is a \mathbb{F}^B -martingale, i.e.,

$$(3.13) \quad \mathcal{M}_t^{u,v} = \mathbb{E}[\mathcal{M}_T^{u,v} | \mathcal{F}_t], \quad t \in [0, T].$$

Proof. For $v \in C^{1,2}$, the Itô formula implies that for $t \in [0, T]$,

$$(3.14) \quad v(t, X_t) = v(0, X_0) + \int_0^t (\partial_t + \mathcal{L})v(s, X_s) ds + \int_0^t \partial_x v \sigma(s, X_s) dB_s.$$

(3.11) \Rightarrow (3.13): Inserting (3.11) into the above equation and further using the definition of (3.4), we obtain

$$\mathcal{M}_t^{u,v} = v(t, X_t) + \int_0^t H^{u,v}(s, X_s) ds = v(0, X_0) + \int_0^t \partial_x v \sigma(s, X_s) dB_s, \quad t \in [0, T],$$

Then $M_t^{u,v}(t, X_t)$ is a martingale from the above equation combined with the first condition in (3.12), thus (3.13) holds.

(3.13) \Rightarrow (3.11): Recalling again the definition in (3.4), the last two conditions in (3.12) implies that $\mathbb{E}[\mathcal{M}_T^{u,v}] < \infty$. Then by the martingale representation theorem [42, Theorem 1.2.9], there exists a \mathbb{F}^B -adapted process $Z : [0, T] \times \Omega \rightarrow \mathbb{R}^q$ such that

$$\mathbb{E} \left[\int_0^T |Z_s|^2 ds \right] < +\infty, \quad \mathcal{M}_t^{u,v} = \mathcal{M}_0^{u,v} + \int_0^t Z_s dB_s, \quad t \in [0, T].$$

By using the definition $\mathcal{M}_t^{u,v}$ in (3.4) above, we then have

$$(3.15) \quad v(t, X_t) = v(0, X_0) - \int_0^t H^{u,v}(s, X_s) ds + \int_0^t Z_s dB_s.$$

Combining (3.14) and (3.15), we have that

$$Q_t := \int_0^t \{(\partial_t + \mathcal{L})v(s, X_s) + H^{u,v}(s, X_s)\} ds = \int_0^t \{\partial_x v \sigma(s, X_s) - Z_s\} dB_s$$

for $t \in [0, T]$, which means that Q is a \mathbb{F}^B -adapted process with finite variation, and is also a continuous martingale with $Q_0 = 0$. Thus it follows from [42, Proposition 1.1.9] that $Q_t = 0$ for any $t \in [0, T]$, a.s., which validates (3.11). \square

Lemmas 3.2 and 3.4 directly lead to the following theorem, which gives the martingale formulation (3.16) for the HJB-type equation (1.1).

THEOREM 3.5. *Assume $(u, v) \in \mathcal{U}_{\text{ad}} \times C^{1,2}$ satisfies (3.7) and (3.12). Then, an optimal feedback control u satisfying (3.8), and the value function v satisfying (1.1) for $t \in [0, T]$ and $x \in \Gamma(X_t)$, can be found by the following two conditions,*

$$(3.16) \quad \int_0^T \mathbb{E}[H_t^{u,v}] dt = \inf_{\bar{u} \in \mathcal{U}_{\text{ad}}} \int_0^T \mathbb{E}[H_t^{\bar{u},v}] dt, \quad \mathcal{M}_t^{u,v} = \mathbb{E}[\mathcal{M}_T^{u,v} | \mathcal{F}_t], \quad t \in [0, T],$$

where $M_t^{u,v}$ and $H_t^{u,v}$ are given by (3.3) and (3.4), respectively.

Remark 3.6. A unique feature of the martingale formulation (3.16) is that it works with expectations and conditional expectations associated with the diffusion process X , rather than its pathwise properties. These expectations can be approximated by applying the Euler-Maruyama scheme [35, Proposition 5.11.1] to (3.2), which achieves a first-order convergence rate in the weak sense (see the numerical results in subsection 4.3). In contrast, related works such as [13, 21, 26, 28, 43, 51, 53] leverage the pathwise properties of X . Consequently, their method depend on the strong convergence rate of the Euler-Maruyama scheme, which is of order $1/2$, as analyzed in [17, 22, 26] and demonstrated numerically in [51].

Now based on Theorem 3.5, the key issue is to fulfill the minimum condition and the martingale condition in (3.16), to be achieved by the SOC-MartNet algorithm.

3.2. SOC-MartNet via adversarial learning for control/value functions.

Under some Lipschitz continuity and boundedness conditions on μ and σ , the uncontrolled diffusion X given by (3.2) is a Markov process relative to \mathbb{F}^B [46, Theorem 17.2.3], which, recalling (3.4), implies that

$$\mathbb{E}[\mathcal{M}_T^{u,v} | \mathcal{F}_t] = \mathbb{E}[\mathcal{M}_T^{u,v} | X_t], \quad t \in [0, T].$$

Thus the martingale condition in (3.16) can be simplified into

$$(3.17) \quad \mathcal{M}_t^{u,v} = \mathbb{E}[\mathcal{M}_T^{u,v} | X_t], \quad t \in [0, T].$$

To avoid computing the conditional expectation $\mathbb{E}[\cdot | X_t]$ as in the original DeepMartNet [5, 6], we modify the martingale condition in (3.17) into

$$(3.18) \quad \sup_{\rho \in \mathcal{T}} \left| \int_0^{T-\Delta t} \mathbb{E}[\rho(t, X_t) (\mathcal{M}_{t+\Delta t}^{u,v} - \mathcal{M}_t^{u,v})] dt \right|^2 = 0,$$

where \mathcal{T} denotes the set of test functions, defined by

$$\mathcal{T} := \{ \rho : [0, T] \times \mathbb{R}^d \rightarrow \mathbb{R} \mid \rho \text{ is smooth and bounded} \},$$

and $\Delta t \in (0, T)$ is the time step size. Here ρ in \mathcal{T} is a general test function. For sufficiently small Δt , the condition (3.18) ensures the martingale condition in (3.17). Actually, by the property of conditional expectations, it holds that

$$(3.19) \quad \mathbb{E} [\rho(t, X_t) (\mathcal{M}_{t+\Delta t}^{u,v} - \mathcal{M}_t^{u,v})] = \mathbb{E} [\rho(t, X_t) \mathbb{E} [(\mathcal{M}_{t+\Delta t}^{u,v} - \mathcal{M}_t^{u,v}) | X_t]]$$

for $t \in [0, T - \Delta t]$. Inserting (3.19) into (3.18), we have that

$$\int_0^{T-\Delta t} \mathbb{E} [\rho(t, X_t) \mathbb{E} [(\mathcal{M}_{t+\Delta t}^{u,v} - \mathcal{M}_t^{u,v}) | X_t]] dt = 0 \quad \text{for all } \rho \in \mathcal{T},$$

where $\mathbb{E} [(\mathcal{M}_{t+\Delta t}^{u,v} - \mathcal{M}_t^{u,v}) | X_t]$ is a deterministic and Borel measurable function of (t, X_t) [34, Corollary 1.97], and thus,

$$(3.20) \quad \mathbb{E} [(\mathcal{M}_{t+\Delta t}^{u,v} - \mathcal{M}_t^{u,v}) | X_t] = 0, \quad (t, \omega) \in [0, T - \Delta t] \times \Omega, \quad \text{a.e.-} dt \times \mathbb{P}.$$

The above conditions imply that $\mathcal{M}^{u,v}$ satisfies the martingale condition in (3.17) approximately for sufficiently small Δt .

A unique feature of (3.18) lies in its natural connection to adversarial learning [50], based on which, we can fulfill the conditions (1.2) and (3.16) by

$$(3.21) \quad (u, v) = \lim_{\lambda \rightarrow +\infty} \arg \min_{(\bar{u}, \bar{v}) \in \mathcal{U}_{\text{ad}} \times \mathcal{V}} \left\{ \sup_{\rho \in \mathcal{T}} \mathbb{L}(\bar{u}, \bar{v}, \rho, \lambda) \right\}$$

where $u \in \mathcal{U}_{\text{ad}}$ given in (2.1), and $v \in \mathcal{V}$ the set of candidate value functions satisfying (1.2), i.e.,

$$(3.22) \quad \mathcal{V} := \{ v : [0, T] \times \mathbb{R}^d \rightarrow \mathbb{R} \mid v \in C^{1,2}, v(T, x) = g(x), \forall x \in \mathbb{R}^d \},$$

and \mathbb{L} is the augmented Lagrangian defined by

$$(3.23) \quad \mathbb{L}(u, v, \rho, \lambda) := \int_0^T \mathbb{E} [H_t^{u,v}] dt + \lambda \left| \int_0^{T-\Delta t} \mathbb{E} [\rho(t, X_t) (\mathcal{M}_{t+\Delta t}^{u,v} - \mathcal{M}_t^{u,v})] dt \right|^2$$

with λ the multiplier being sufficiently large.

For adversarial learning, we replace the functions u, v and ρ by the control network $u_\alpha : [0, T] \times \mathbb{R}^d \rightarrow U$, the value network $v_\theta : [0, T] \times \mathbb{R}^d \rightarrow \mathbb{R}$ and the adversarial network $\rho_\eta : [0, T] \times \mathbb{R}^d \rightarrow \mathbb{R}^r$ parameterized by α, θ and η , respectively. Since the range of u_α should be restricted in the control space U , if $U = [a, b] := \prod_{i=1}^m [a_i, b_i]$ with a_i, b_i the i -th elements of $a, b \in \mathbb{R}^m$, the structure of u_α can be

$$(3.24) \quad u_\alpha(t, x) = a + \frac{b-a}{6} \text{ReLU6}(\psi_\alpha(t, x)), \quad (t, x) \in [0, T] \times \mathbb{R}^d,$$

where $\text{ReLU6}(y) := \min\{\max\{0, y\}, 6\}$ is an activation function and $\psi_\alpha : [0, T] \times \mathbb{R}^d \rightarrow \mathbb{R}^m$ is a neural network with parameter α . Remark 3.7 provides a penalty method to deal with general control spaces. To fulfill the terminal condition in (3.22), the value network v_θ takes the form of

$$v_\theta(T, x) := g(x), \quad v_\theta(t, x) := \phi_\theta(t, x) \quad \text{for } t \in [0, T], \quad x \in \mathbb{R}^d,$$

where $\phi_\theta : [0, T] \times \mathbb{R}^d \rightarrow \mathbb{R}$ a neural network parameterized by θ .

The adversarial network ρ_η plays the role of test functions. By our experiment results, ρ_η is not necessarily to be very deep, but instead, it can be a shallow network with enough output dimensionality. A typical example is that

$$(3.25) \quad \rho_\eta(t, x) = \sin(W_1 t + W_2 x + b) \in \mathbb{R}^r, \quad \eta := (W_1, W_2, b) \in \mathbb{R}^r \times \mathbb{R}^{r \times d} \times \mathbb{R}^r$$

for $(t, x) \in [0, T] \times \mathbb{R}^d$, where $\sin(\cdot)$ is the activation function applied on $W_1 t + W_2 x + b$ in an element-wise manner.

SOC-MartNet. Based on (3.21) and (3.23) with $(u_\alpha, v_\theta, \rho_\eta)$ in place of (u, v, ρ) , the solution (u, v) of (3.21) can be approximated by $(u_{\alpha^*}, v_{\theta^*})$ given by

$$(3.26) \quad (\alpha^*, \theta^*) = \lim_{\lambda \rightarrow +\infty} \arg \min_{\alpha, \theta} \left\{ \max_{\eta} L(\alpha, \theta, \eta, \lambda) \right\},$$

where

$$(3.27) \quad L(\alpha, \theta, \eta, \lambda) := \int_0^T \mathbb{E} [H_t^{u_\alpha, v_\theta}] dt + \lambda \left| \int_0^{T-\Delta t} \mathbb{E} [\rho_\eta(t, X_t) (\mathcal{M}_{t+\Delta t}^{u_\alpha, v_\theta} - \mathcal{M}_t^{u_\alpha, v_\theta})] dt \right|^2$$

with H^{u_α, v_θ} and M^{u_α, v_θ} given in (3.3) and (3.4), respectively. The proposed method will be named SOC-MartNet for SOCPs as it is based on the martingale condition of the cost process (3.13), similar to the DeepMartNet [5, 6].

Remark 3.7. If the control space U is general rather than an interval, the network structure in (3.24) is no longer applicable. This issue can be addressed by appending a new penalty term on the right side of (3.27) to ensure $u_\alpha(t, X_t)$ remains within U . The following new loss function is an example:

$$\bar{L}(\alpha, \theta, \eta, \lambda, \bar{\lambda}) := L(\alpha, \theta, \eta, \lambda) + \bar{\lambda} \int_0^T \mathbb{E} [\text{dist}(u_\alpha(t, X_t), U)] dt,$$

where $L(\alpha, \theta, \eta, \lambda)$ is given in (3.27); $\bar{\lambda} \geq 0$ is a multiplier and $\text{dist}(\kappa, U)$ denotes a certain distance between $\kappa \in \mathbb{R}^m$ and U .

3.3. Training algorithm. To solve (3.26) numerically, we introduce a time partition on the time interval $[0, T]$, i.e.,

$$\pi_N := \{t_0, t_1, \dots, t_N\} \text{ s.t. } 0 = t_0 < t_1 < t_2 < \dots < t_n < t_{n+1} < \dots < t_N = T.$$

For $n = 0, 1, \dots, N-1$, denote $\Delta t_n := t_{n+1} - t_n$ and $\Delta B_{n+1} := B_{n+1} - B_n$. Then we apply the following numerical approximations on the loss function in (3.27):

1. The process $(X_{t_n})_{n=0}^N$ can be approximated by $(X_n)_{n=0}^N$, which is obtained by applying the Euler scheme to the SDE (3.2), i.e., for $n = 0, 1, 2, \dots, N-1$,

$$(3.28) \quad X_{n+1} = X_n + \mu(t_n, X_n) \Delta t_n + \sigma(t_n, X_n) \Delta B_{n+1}.$$

2. The integral in (3.4) can be approximated by quadrature rules, e.g., the trapezoid formula, which leads to $\mathcal{M}_{t_{n+1}}^{u_\alpha, v_\theta} - \mathcal{M}_{t_n}^{u_\alpha, v_\theta} \approx \Delta \mathcal{M}_{n+1}^{\alpha, \theta}$ with

$$\begin{aligned} \Delta \mathcal{M}_{n+1}^{\alpha, \theta} &:= v_\theta(t_{n+1}, X_{n+1}) - v_\theta(t_n, X_n) - \frac{1}{2} (H_n^{\alpha, \theta} + H_{n+1}^{\alpha, \theta}) \Delta t_n, \\ H_n^{\alpha, \theta} &:= H(t_n, X_n, u_\alpha(t_n, X_n), \partial_x v_\theta(t_n, X_n), \partial_{xx}^2 v_\theta(t_n, X_n)). \end{aligned}$$

3. The expectations in (3.27) can be approximated by the Monte-Carlo method based on the i.i.d. samples of $\{(X_n, H_n^{\alpha, \theta}, \Delta \mathcal{M}_n^{\alpha, \theta})\}_{n=0}^N$, i.e.,

$$(3.29) \quad \{(X_n^{(m)}, H_n^{\alpha, \theta, (m)}, \Delta \mathcal{M}_n^{\alpha, \theta, (m)})\}_{n=0}^N, \quad m = 1, 2, \dots, M.$$

Combining the above approximations, the loss function in (3.27) is replaced by its mini-batch version for stochastic gradient descent or ascent,

$$(3.30) \quad L(\alpha, \theta, \eta, \lambda; A) := \frac{1}{|A|} \sum_{(n, m) \in A} H_n^{\alpha, \theta, (m)} \Delta t_n + \lambda |G(\alpha, \theta, \eta, \lambda; A)|^2,$$

$$(3.31) \quad G(\alpha, \theta, \eta; A) := \frac{1}{|A|} \sum_{(n, m) \in A} \rho_\eta(t_n, X_n^{(m)}) \Delta \mathcal{M}_{n+1}^{\alpha, \theta, (m)} \Delta t_n$$

with $\Delta t_N := \Delta \mathcal{M}_{N+1}^{\alpha, \theta} := 0$ for convenience, where A is a index subset randomly taken from $\{0, 1, \dots, N\} \times \{1, 2, \dots, M\}$ and is updated at each optimization step. The loss function in (3.30) can be optimized by alternating gradient descent and ascent of $L(\alpha, \theta, \eta, \lambda; A)$ over (α, θ) and (λ, η) , respectively. The details are presented in Algorithm 3.1.

Remark 3.8. In the martingale formulation, the diffusion process X_t given by (3.2) is fixed and independent of the control and the value function, and thus its sample paths can be generated offline before optimizing the loss function in (3.30). Moreover, in the SOC-MartNet, the gradient computation for the loss function and the training of neural networks are both free of recursive iterations along the time direction, which contributes to significant efficiency gains for the SOC-MartNet. This feature is different from many existing deep-learning probabilistic methods for PDEs, e.g., [1, 13, 25, 26, 28, 40, 51, 53]. Our numerical experiments in subsection 4.8 confirm the high efficiency of the SOC-MartNet.

3.4. Application to parabolic problems. The SOC-MartNet proposed in the last subsection is applicable for the HJB-type equation (1.1). In this section, we explore how SOC-MartNet can be tailored to parabolic equations, yielding enhanced efficiency and simplicity. Specifically, we consider the parabolic equation in the form of

$$(3.32) \quad \partial_t v(t, x) + \mathcal{L}v(t, x) + f(t, x, v(t, x), \partial_x v(t, x), \partial_{xx}^2 v(t, x)) = 0$$

with f being a given function. Here f could depend also on $v(t, x)$, compared with \bar{H} in (3.1), and this dependence does not pose any difficulties in applying the method to (3.32).

By (3.4) with f in place of H , we obtain a new cost process $\tilde{\mathcal{M}}^v$ independent of u , i.e.,

$$\tilde{\mathcal{M}}_t^v := v(t, X_t) + \int_0^t f(s, X_s, v(s, X_s), \partial_x v(s, X_s), \partial_{xx}^2 v(s, X_s)) ds, \quad t \in [0, T].$$

Under some regularity conditions, by following the deductions in section 3.1, we conclude that v satisfies the equation (1.1) for $t \in [0, T]$ and $x \in \Gamma(X_t)$ if $\tilde{\mathcal{M}}^v$ is a \mathbb{F}^B -martingale. Thus the value function v_{θ^*} can be learned through adversarial training to enforce the martingale property of $\tilde{\mathcal{M}}^v$, i.e.,

$$(3.33) \quad \theta^* = \arg \min_{\theta} \left\{ \max_{\eta} |\tilde{G}(\theta, \eta)| \right\}$$

Algorithm 3.1 SOC-MartNet for solving the HJB-type equation (1.1)

Input: I : the maximum number of iterations of stochastic gradient algorithm; M : the total number of sample paths of diffusion process from (3.28); $\delta_1/\delta_2/\delta_3/\delta_4$: learning rates for control network u_α /value network v_θ /adversarial network ρ_η /multiplier λ ; $\bar{\lambda}$: upper bound of multiplier λ ; J/K : number of $(\alpha, \theta)/(\lambda, \eta)$ updates per iteration.

- 1: Initialize the networks u_α , v_θ , ρ_η and the multiplier λ
 - 2: Generate the sample paths $\{X_n^{(m)}\}_{n=0}^N$ for $m = 1, 2, \dots, M$ by (3.28)
 - 3: **for** $i = 0, 1, \dots, I - 1$ **do**
 - 4: Sample the index subset $A_i \subset \{0, 1, \dots, N - 1\} \times \{1, 2, \dots, M\}$ per (4.1)
 - 5: **for** $j = 0, 1, \dots, J - 1$ **do**
 - 6: $\alpha \leftarrow \alpha - \delta_1 \nabla_\alpha L(\alpha, \theta, \eta, \lambda; A_i)$ // L is computed by (3.30)
 - 7: $\theta \leftarrow \theta - \delta_2 \nabla_\theta L(\alpha, \theta, \eta, \lambda; A_i)$
 - 8: **end for**
 - 9: **for** $k = 0, 1, \dots, K - 1$ **do**
 - 10: $\eta \leftarrow \eta + \delta_3 \nabla_\eta L(\alpha, \theta, \eta, \lambda; A_i)$
 - 11: $\lambda \leftarrow \min \{\bar{\lambda}, \lambda + \delta_4 |G(\alpha, \theta, \eta; A_i)|^2\}$ // G is computed by (3.31)
 - 12: **end for**
 - 13: **end for**
- Output:** u_α and v_θ

with

$$\tilde{G}(\theta, \eta) := \int_0^{T-\Delta t} \mathbb{E} \left[\rho_\eta(t, X_t) \left(\tilde{\mathcal{M}}_{t+\Delta t}^{v_\theta} - \tilde{\mathcal{M}}_t^{v_\theta} \right) \right] dt.$$

To learn the value function from (3.33), at each iteration step, the loss function $\tilde{G}(\theta, \eta)$ is replaced by its mini-batch version defined as

$$(3.34) \quad \tilde{G}(\theta, \eta; A) := \frac{1}{|A|} \sum_{(n,m) \in A} \rho_\eta(t_n, X_n^{(m)}) \Delta \tilde{\mathcal{M}}_{n+1}^{\theta, (m)} \Delta t_n,$$

where A is a index subset randomly taken from $\{0, 1, \dots, N\} \times \{1, 2, \dots, M\}$ and

$$\begin{aligned} \Delta \tilde{\mathcal{M}}_{n+1}^{\theta, (m)} &:= v_\theta(t_{n+1}, X_{n+1}^{(m)}) - v_\theta(t_n, X_n^{(m)}) - \frac{1}{2} \left(f_n^{\theta, (m)} + f_{n+1}^{\theta, (m)} \right) \Delta t_n, \\ f_n^{\theta, (m)} &:= f \left(t_n, X_n^{(m)}, v_\theta(t_n, X_n^{(m)}), \partial_x v_\theta(t_n, X_n^{(m)}), \partial_{xx}^2 v_\theta(t_n, X_n^{(m)}) \right), \end{aligned}$$

and $X_n^{(m)}$ is introduced in (3.29). Algorithm 3.2 presents the detailed procedures of the SOC-MartNet for parabolic equations.

4. Numerical tests. In this section, we carry out numerical tests to show the behaviors of the SOC-MartNet in solving high-dimensional parabolic equations and HJB equations.

Sampling of index set A_i . For the SOC-MartNet given by Algorithms 3.1 and 3.2, the index subset A_i on Line 4 is taken as

$$(4.1) \quad A_i = \{0, 1, 2, \dots, N\} \times M_i,$$

where M_i is a random subset of the index set $\{1, 2, \dots, M\}$ and obtained as follows:

Algorithm 3.2 SOC-MartNet for solving the parabolic equation (3.32)

Input: I : the maximum number of iterations of stochastic gradient algorithm; M : the total number of sample paths of diffusion process from (3.28); δ_2/δ_3 : learning rates for value network v_θ /adversarial network ρ_η ; J/K : number of θ/η updates per iteration.

```

1: Initialize the networks  $v_\theta$  and  $\rho_\eta$ 
2: Generate the sample paths  $\{X_n^{(m)}\}_{n=0}^N$  for  $m = 1, 2, \dots, M$  by (3.28)
3: for  $i = 0, 1, \dots, I - 1$  do
4:   Sample the index subset  $A_i \subset \{0, 1, \dots, N - 1\} \times \{1, 2, \dots, M\}$  per (4.1)
5:   for  $j = 0, 1, \dots, J - 1$  do
6:      $\theta \leftarrow \theta - \delta_2 \nabla_\theta \left| \tilde{G}(\theta, \eta; A_i) \right|^2$  //  $\tilde{G}$  is computed by (3.34)
7:   end for
8:   for  $k = 0, 1, \dots, K - 1$  do
9:      $\eta \leftarrow \eta + \delta_3 \left| \nabla_\eta \tilde{G}(\theta, \eta; A_i) \right|^2$ 
10:  end for
11: end for
Output:  $v_\theta$ 

```

1. At the beginning of each epoch, a random permutation of $\{1, 2, \dots, M\}$ is created and equally split into some index subsets P_1, P_2, \dots, P_m ;
2. During the epoch, P_1, P_2, \dots, P_m are used as M_i one-by-one for each iteration;
3. Once all the index subsets have been used, namely the epoch is completed, the process restarts at step 1 for the next epoch.

At the i -th iteration step, we take the batch size $|M_i|$ of sample paths as $|M_i| = 256$ and 128 for $d \leq 1000$ and $d > 1000$, respectively.

The numerical method solves $v(0, x)$ for $x \in D_0$, where D_0 is a set of finite spatial points in \mathbb{R}^d and will be specified in each benchmark problem. The start points $X_0^{(m)}$ of the sample paths in (3.28) are randomly taken from the set D_0 with replacement, where the total number of sample paths is set to $M = 10^5$.

If no otherwise specified, we take $T = 1$ and $N = 100$ for all involved loss functions, and all the loss functions are minimized by the RMSProp algorithm. The learning rates on Lines 6, 7 and 10 of Algorithm 3.1 are set to

$$\delta_1 = \delta_2 = \delta_0 \times 10^{-3} \times 0.01^{i/I}, \quad \delta_3 = 10^{-2} \times 0.01^{i/I}, \quad i = 0, 1, \dots, I - 1$$

with $\delta_0 := 3d^{-0.5}$ for $d \leq 1000$ and $\delta_0 := 3d^{-0.8}$ for $d > 1000$. If not otherwise specified, the initial value of λ is 10 with its learning rate $\delta_4 = 10$ and its upper bound $\bar{\lambda}$ set to 10^3 . The inner iteration steps are $J = 2K = 2$. The neural networks u_α and v_θ both consist of 6 hidden layers with $d + 10$ ReLU units in each hidden layer. The adversarial network ρ_η is given by (3.25) with the output dimensionality $r = 600$.

All the tests are implemented by Python 3.12 and PyTorch 2.51. If no otherwise specified, the algorithm is accelerated by the strategy of Distributed Data Parallel (DDP) ¹ on a compute node equipped with 8 GPUs (NVIDIA A100-SXM4-80GB).

¹https://github.com/pytorch/tutorials/blob/main/intermediate_source/ddp_tutorial.rst

When reporting the numerical results, “SD”, “vs” and “Iter.” are short for “standard deviation”, “versus” and “Iter.”, respectively. The term “Mart. Loss” denotes the value of $|G(\alpha, \theta, \eta; A_i)|^2$ defined in (3.31), and “Hamilt.” denotes the empirical Hamiltonian defined by $\text{Hamilt.} := |A_i|^{-1} \sum_{(n,m) \in A_i} H_n^{\alpha, \theta, (m)} \Delta t_n$ recalling (3.30). The relative L^1 -error and L^∞ -error are respectively defined by

$$\begin{aligned} \text{Rel. } L^1\text{-error} &:= \left(\sum_{x \in D_0} |\widehat{v}(0, x) - v(0, x)| \right) / \left(\sum_{x \in D_0} |v(0, x)| \right), \\ \text{Rel. } L^\infty\text{-error} &:= \left(\max_{x \in D_0} |\widehat{v}(0, x) - v(0, x)| \right) / \left(\max_{x \in D_0} |v(0, x)| \right). \end{aligned}$$

4.1. Linear parabolic problem. We consider the following problem:

$$(4.2) \quad \begin{cases} (\partial_t + \frac{1}{2} \Delta_x) v(t, x) - f(t, x) = 0, & (t, x) \in [0, T] \times \mathbb{R}^d, \\ v(T, x) = g(x), & x \in \mathbb{R}^d, \end{cases}$$

where f and g are chosen such that v is given by

$$(4.3) \quad v(t, x) = 1 + \frac{1}{d} \sum_{i=1}^d \sin(t + x_i), \quad (t, x) \in [0, T] \times \mathbb{R}^d.$$

We apply the SOC-MartNet (Algorithm 3.2) to solve $v(0, x)$ for $x \in D_0$, where D_0 consists of M uniformly spaced grid points on the two spatial line segments $S_1 \cup S_2$ defined by

$$(4.4) \quad S_1 := \{s \mathbf{e}_1 : s \in [-1, 1]\}, \quad \mathbf{e}_1 := (1, 0, 0, \dots, 0)^\top \in \mathbb{R}^d,$$

$$(4.5) \quad S_2 := \{s \mathbf{1}_d : s \in [-1, 1]\}, \quad \mathbf{1}_d := (1, 1, \dots, 1)^\top \in \mathbb{R}^d.$$

The relevant numerical results for $d = 100, 1000, 2000$ are presented in Figure 1, which demonstrate that the SOC-MartNet is effective for problems with dimensionality upto 2000.

4.2. Semilinear parabolic equation. We consider the semilinear parabolic equation from [13, Section 4.3]:

$$(4.6) \quad \begin{cases} (\partial_t + \Delta_x) v(t, x) - |\partial_x v(t, x)|^2 = 0, & (t, x) \in [0, T] \times \mathbb{R}^d, \\ v(T, x) = 1 + g(x), & x \in \mathbb{R}^d \end{cases}$$

for some given terminal function $g : \mathbb{R}^d \rightarrow \mathbb{R}$. The problem (4.6) admits an analytic solution as

$$(4.7) \quad v(t, x) = 1 - \ln \left(\mathbb{E} \left[\exp \left(-g(x + \sqrt{2} B_{T-t}) \right) \right] \right), \quad (t, x) \in [0, T] \times \mathbb{R}^d.$$

To compute the absolute error of numerical solutions, the analytic solution in (4.7) is approximated by the Monte-Carlo method applied on the expectation using 10^6 i.i.d. samples of B_{T-t} .

For this example, we consider an oscillatory terminal function as

$$(4.8) \quad g(x) := \frac{1}{d} \sum_{i=1}^d \left\{ \sin(x_i - \frac{\pi}{2}) + \sin \left((\epsilon_0 + x_i^2)^{-1} \right) \right\}, \quad x \in \mathbb{R}^d, \quad \epsilon_0 = \pi/10.$$

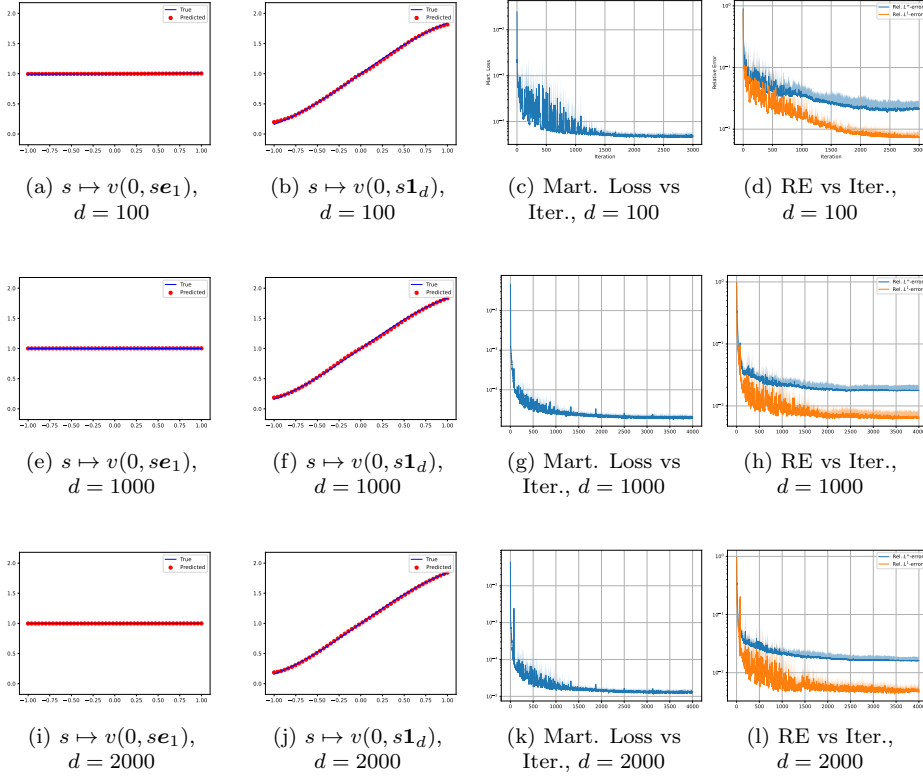


Fig. 1: Numerical results of SOC-MartNet (Algorithm 3.2) for the linear parabolic problem (4.2). The shaded region represents the mean + $2 \times$ SD of the loss values and relative errors across 5 independent runs. The running times are 37, 112 and 363 seconds for $d = 100$, 1000, and 2000, respectively.

Under (4.8), the true solution along the diagonal of the unite cube, i.e., $s \mapsto v(t, s\mathbf{1}_d)$, is independent of the spatial dimensionality d , whose graphs at $t = 0$ and T are presented in Figures 2 (a) - (d). As the graphs show, although $s \mapsto v(T, s\mathbf{1}_d)$ is oscillatory around $s = 0$, the curve of $s \mapsto v(0, s\mathbf{1}_d)$ is relatively smooth and depends on the terminal time T .

We apply the SOC-MartNet (Algorithm 3.2) to solve $v(0, x)$ for $x \in D_0$ with D_0 the same as the last example. The relevant numerical results for $d = 100$ are presented in Figures 2 (e) - (h), which show that the SOC-MartNet (Algorithm 3.2) remains unaffected by the oscillations in $g(x)$, and captures the analytical solution well.

4.3. Test on time convergence rate. We consider a specific parabolic equation (3.32) with a variable coefficient in \mathcal{L} and an Allen-Cahn-type source term f , i.e.,

$$(4.9) \quad \mathcal{L} = \sum_{i=1}^d \sin(2x_i) \partial_{x_i} + \frac{1}{2} \sum_{i=1}^d (1 + 0.5 \sin(5t + x_i))^2 \partial_{x_i}^2,$$

$$f(t, x, v, \partial_x v, \partial_{xx}^2 v) = v - v^3 + \bar{f}(t, x),$$

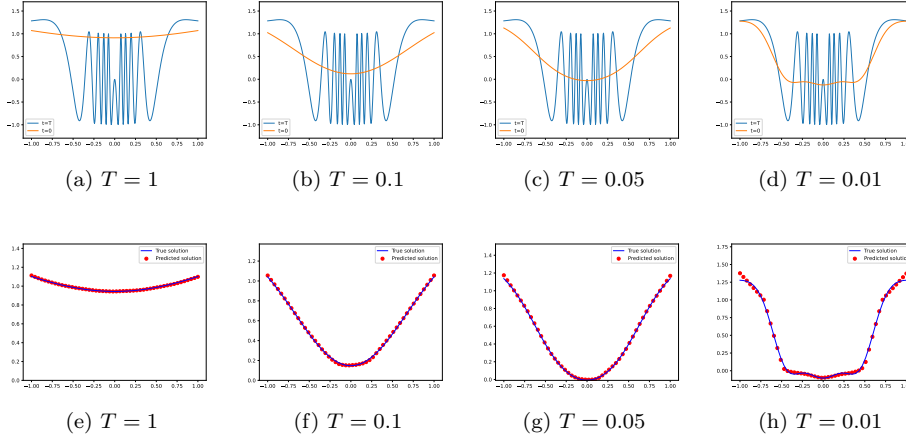


Fig. 2: Numerical results of SOC-MartNet (Algorithm 3.2) for the semilinear parabolic problem (4.6) with $d = 100$ and oscillatory terminal function (4.8). (a) - (d) Graphs of the true solutions $s \mapsto v(t, s\mathbf{1}_d)$ at $t = 0, T$ with varying T . (e) - (h) Numerical solution of $s \mapsto v(0, s\mathbf{1}_d)$ given by the SOC-MartNet.

where the function \bar{f} and the terminal condition $v(T, x) = g(x)$ are chosen such that the true solution is given by (4.3). The relevant numerical results of SOC-MartNet (Algorithm 3.2) are shown in Figure 3. The relative error RE_1 closely aligns with the red reference line with slope 1.01, indicating a first-order convergence rate of $O(N^{-1.01})$, and in line with our claim in Remark 3.6.

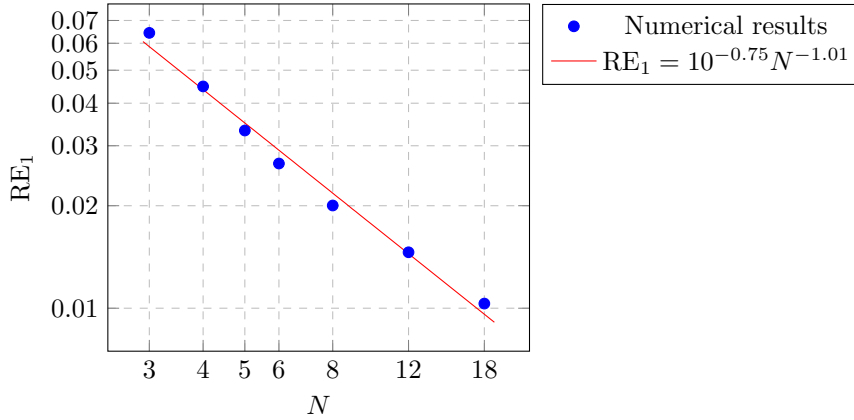


Fig. 3: Log-log plot of the relative L^1 -error RE_1 of SOC-MartNet (Algorithm 3.2) vs the number of time partitions N for the parabolic equation (3.32) with parameter setting (4.9) and with $d = 100$. The red reference line indicates a first-order convergence rate of $O(N^{-1.01})$.

4.4. Non-degenerated HJB equation without using explicit form of $\inf_u H$. We consider the following HJB equation [1, Section 3.1]:

$$(4.10) \quad \begin{cases} (\partial_t + b^\top \partial_x + \epsilon_1 \Delta_x) v(t, x) + \inf_{\kappa \in \mathbb{R}^d} (2\kappa^\top \partial_x v(t, x) + c_1 |\kappa|^2) = 0 \\ v(T, x) = g(x), \quad g(x + b) := \frac{1}{d} \sum_{i=1}^d \left\{ \sin(x_i - \frac{\pi}{2}) + \sin((\epsilon_0 + x_i^2)^{-1}) \right\} \end{cases}$$

with $(t, x) \in [0, T] \times \mathbb{R}^d$, where $b \in \mathbb{R}^d$, c_1, ϵ_0 and $\epsilon_1 > 0$ are parameters to be specified. The HJB equation (4.10) is associated with the SOCP:

$$(4.11) \quad u^* = \arg \min_{u \in \mathcal{U}_{\text{ad}}} J(u), \quad J(u) := 1 + \mathbb{E} \left[\int_0^T c_1 |u_s|^2 ds + g(X_T^u) \right],$$

$$\mathcal{U}_{\text{ad}} = \{u : [0, T] \times \Omega \rightarrow \mathbb{R}^d : u \text{ is } \mathbb{F}^B\text{-adapted}\},$$

$$(4.12) \quad X_t^u = X_0 + \int_0^t (b + 2u_s) ds + \int_0^t \sqrt{2\epsilon_1} dB_s, \quad t \in [0, T],$$

where B is a d -dimensional standard Brownian motion. For this example, we take $c_1 = \epsilon_1^{-2}$ such that the HJB (1.1) admits an analytic solution given by

$$(4.13) \quad v(t, x) = -\ln(\mathbb{E}[\exp(-g(X_T^{t,x}))]), \quad X_T^{t,x} := x + (T - t)b + \sqrt{2\epsilon_1} B_{T-t}.$$

The specific case of the HJB equation (4.10), the associated SOCP (4.11) and parabolic counterpart (4.6), have been used often as benchmark problems in related literature, e.g., [1, 13, 21, 23, 24, 28, 43, 48]. However, most studies have focused on the terminal function $g(x) = \ln(0.5(1 + |x|^2))$, resulting in a smooth exact solution v with inherent low-dimensional structure. In this work, we consider a more complicated $g(x)$ given in (4.10), under which the exact solution $x \mapsto v(t, x)$ is anisotropic along spatial dimensions and highly oscillatory around $t = T$; see Figure 2. Thus this example can effectively demonstrate the ability of numerical methods to address complex high-dimensional problems.

In the numerical tests, specific settings of (4.10) are considered. By selecting different values of b , ϵ_0 , and ϵ_1 , three particular instances of (4.10) are obtained:

- HJB-1: $b = (0, 0, \dots, 0)^\top \in \mathbb{R}^d$, $\epsilon_0 = 0.1\pi$, $\epsilon_1 = 1$.
- HJB-2: $b = (1, 1, \dots, 1)^\top \in \mathbb{R}^d$, $\epsilon_0 = 0.3\pi$, $\epsilon_1 = 0.2$;
- HJB-3: $b = (1, 1, \dots, 1)^\top \in \mathbb{R}^d$, $\epsilon_0 = 0.3\pi$, $\epsilon_1 = 0.1$.

With the optimal control in (4.10) explicitly solved, HJB-1 reduces to the semilinear parabolic equation (4.6). HJB-2 and HJB-3 are more intricate variants of HJB-1, featuring a non-zero drift coefficient b and a smaller ϵ_1 . As shown in Figure 5, the solutions $x \mapsto v(t, x)$ of HJB-2 and -3 remains oscillatory at $t = 0$, even for $T = 1$.

The SOC-MartNet (Algorithm 3.1) is applied to HJB-1 to -3, where no explicit form is used for $\inf_{\kappa \in U} H$, and the optimal control u^* is approximated by the neural network u_α . The numerical method solves $v(0, x)$ for $x \in D_0$ with D_0 consists of M uniformly spaced grid points on $S_2 \cup S_3$, where S_2 is the line segment defined in (4.5) and $S_3 := \{\mathbf{l}(s) : s \in [-1, 1]\}$ is a space curve in \mathbb{R}^d with

$$(4.14) \quad \mathbf{l}(s) := (l_1, l_2, \dots, l_d)^\top \in \mathbb{R}^d, \quad l_i := s \times \text{sgn}(\sin(i)) + \cos(i + \pi s), \quad s \in \mathbb{R},$$

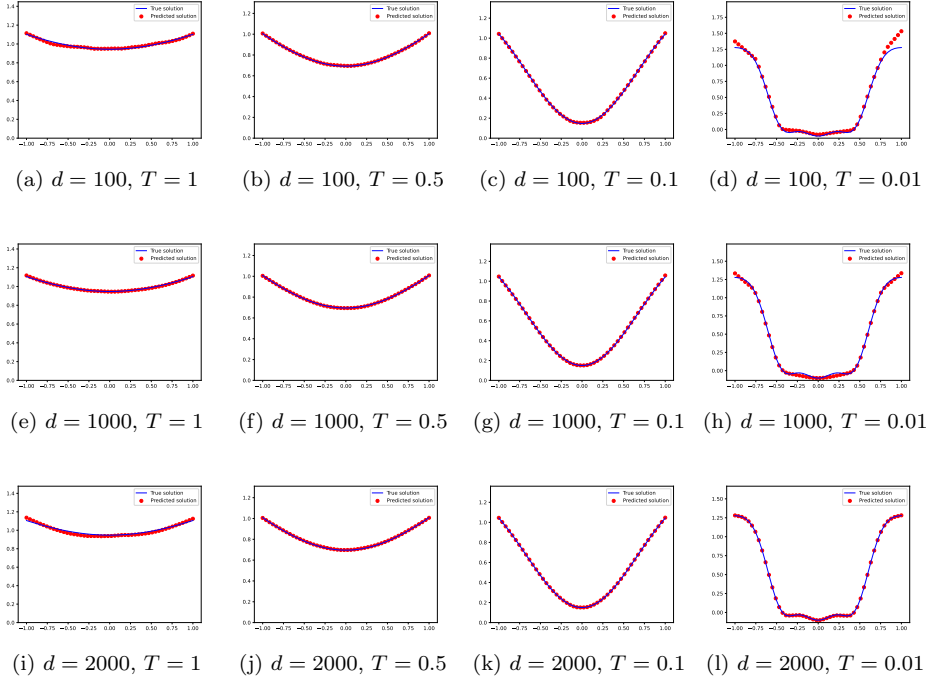


Fig. 4: Graphs of the true solution and the numerical solution of SOC-MartNet for $s \mapsto v(t, s\mathbf{1}_d)$ at $t = 0$ given by HJB-1.

and $\text{sgn}(z) := -1, 0, 1$ for $z < 0, = 0$ and > 0 , respectively. For $d \geq 1000$, the upper bound $\bar{\lambda}$ on Line 11 of Algorithm 3.1 is specially set to 100 for $T = 0.01$ and set to 10^3 for $T = 0.1, 0.5, 1$. The relevant numerical results and some of the convergence histories are presented in Figures 4 and 5.

As the numerical results show, even without using the explicit form of $\inf_{\kappa \in U} H$, the SOC-MartNet (Algorithm 3.1) still works well for the HJB equation with oscillatory and anisotropic terminal function, and with d up to 10^4 .

4.5. Validity of SOC-MartNet solution in space-time region. To illustrate the generalization of our method, we present Figure 6 for HJB-2 with $d = 1000$. The SOC-MartNet solutions remain close to the exact solution for (t, x) outside the time-space region given by $t = 0$ and $x \in D_0$. The relative error on the sample paths $\{X_n\}_{n=0}^N$ grows slightly with t as expected given that the variance of X_t increases over time, causing sparser path distributions. Despite this, the relative errors remain satisfactory across the entire time interval, indicating that SOC-MartNet performs well in the region explored by X_t .

4.6. SOCP with a shifted target. We consider a SOCP with a shifted target function in the terminal condition whose minimum is away from the origin as considered in [38]. Specifically, the considered SOCP is given by (4.11) with $T = 1, b = 0$,

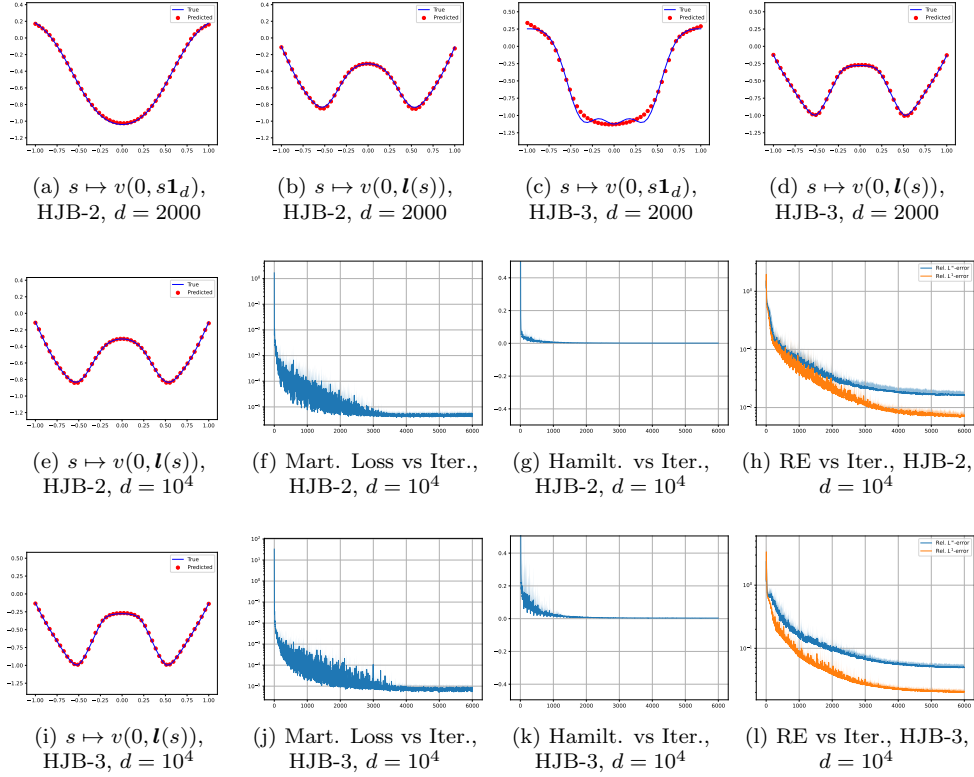


Fig. 5: Numerical results of SOC-MartNet (Algorithm 3.1) for HJB-2 and HJB-3 with $T = 1$ and $d = 2000, 10000$. The shaded region represents the mean $+ 2 \times$ SD of the plotted values across 5 independent runs.

and with the terminal function g replaced by

$$(4.15) \quad g(x) = C_g \ln \left(0.5 \left(1 + \sum_{i=1}^d (x_i - 3)^2 \right) \right),$$

where we set $C_g = 10$ so the exact solution expression (4.13) will not have an overflow issue. The terminal function encourages the control u to drive the state process X_t^u to get close to the target point $(3, 3, \dots, 3)^\top \in \mathbb{R}^d$ at the terminal time. To avoid trivial solutions caused by noise-dominated state equations, we take a small diffusion coefficient as $\epsilon_1 = 0.1$ in (4.12).

We apply the SOC-MartNet (Algorithm 3.1) to solve $v(0, x)$ for $x \in D_0$, where D_0 consists of M uniformly spaced grid points on the line segment S_2 defined in (4.5). At each iteration, we record the empirical values of $J(u_\theta)$, which are estimated via Monte Carlo sampling based on 256 sample paths of the state process in (2.2) approximated by the Euler-Maruyama method with $x_0 = 0$. The relevant numerical results for $d = 100$ and 500 are presented in Figure 7, which shows that the SOC-MartNet provides accurate solutions for the value function. Moreover, the cost value of u_θ quickly converges to the theoretical lower bound $J(u^*) := v(0, x_0)$.

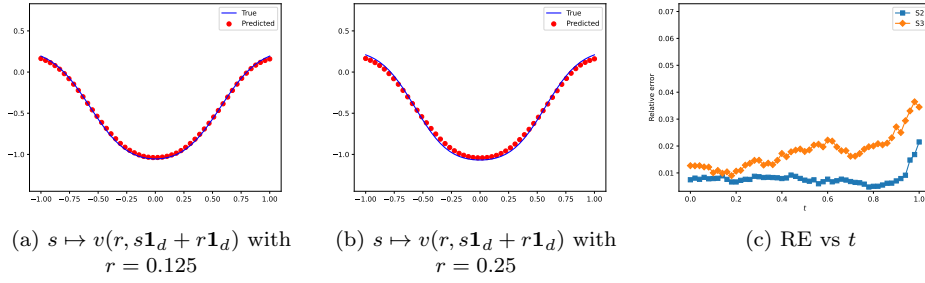


Fig. 6: (a) (b) Numerical solutions of SOC-MartNet (Algorithm 3.1) for HJB-2 with $d = 1000$ and $s \in [-1, 1]$. (c) The RE of the solution along on 8 paths of the process $\{X_n\}_{n=0}^N$ given by (3.28) with $X_0 = 0$ for S2, and $X_0 = \mathbf{l}(0.75)$ for S3.

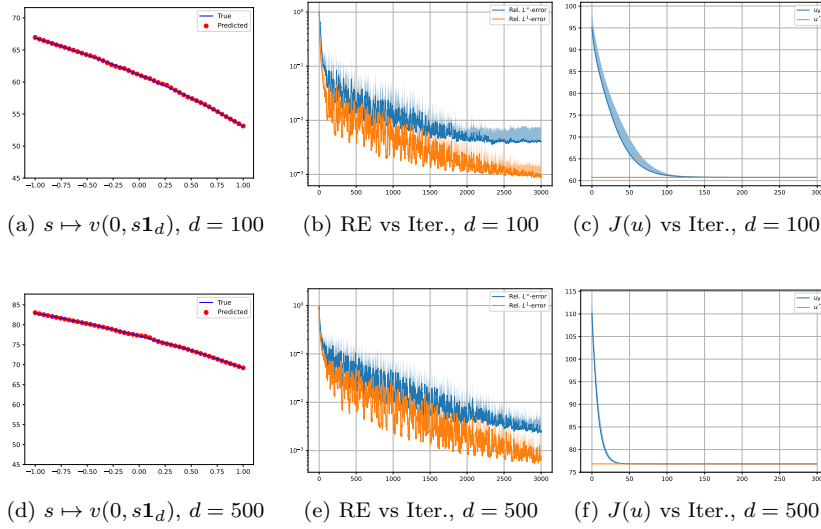


Fig. 7: Numerical results of SOC-MartNet (Algorithm 3.1) for the SOCP with a shifted target in subsection 4.6. The shaded region represents the mean $\pm 2 \times$ SD of the plotted values across 5 independent runs.

4.7. Non-degenerated HJB equation without explicit $\inf_u H$. The $\inf_u H$ in the HJB equation (4.10) in fact has an explicit expression, so to obtain a HJB equation without an explicit form of $\inf_u H$, we modify it by an perturbation of a nonlinear term $\varepsilon \sin(\mathbf{1}_d^\top \kappa)$ to the Hamiltonian, i.e.,

$$(4.16) \quad (\partial_t + b^\top \partial_x + \epsilon_1 \Delta_x) v(t, x) + \inf_{\kappa \in \mathbb{R}^d} \left(2\kappa^\top \partial_x v(t, x) + c_1 |\kappa|^2 + \varepsilon \sin(\mathbf{1}_d^\top \kappa) \right) = 0$$

where $\mathbf{1}_d$ is given in (4.5); ε is a scalar parameter to be specified, and other parameter settings are the same as HJB-2 introduced in subsection 4.4.

Compared with (4.10), the Hamiltonian in (4.16) has no closed-form minimization

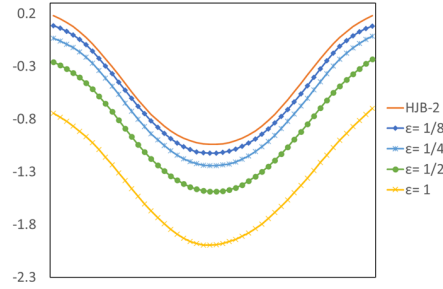


Fig. 8: Numerical results of SOC-MartNet (Algorithm 3.1) for $s \mapsto v(0, s\mathbf{1}_d)$, $s \in [-1, 1]$ from (4.16) with $d = 1000$ and $\varepsilon = 1, 1/2, 1/4, 1/8$ (from bottom up). The top orange curve without markers is the reference solution of HJB-2 (i.e. $\varepsilon = 0$).

due to the added nonlinear term. Consequently, this example can be used to test the effectiveness of SOC-MartNet for general problems. In the tests, we use a decreasing sequence of the perturbation parameter $\varepsilon = 1, 1/2, 1/4, 1/8$, and the solution of (4.16) is expected to approach HJB-2 as ε decreases. Hence, the solution of HJB-2 (i.e., $\varepsilon = 0$) is taken as a reference to evaluate the numerical results of SOC-MartNet for (4.16). The relevant numerical results are presented in Figure 8, where we can see that the solution provided by SOC-MartNet indeed approaches to the reference solution as ε decreases.

4.8. Test on efficiency. Finally, we investigate the efficiency of our method in comparison with the deep BSDE proposed by [13, 21] as a benchmark method. We apply the SOC-MartNet (Algorithm 3.1) and the deep BSDE to solve $v(0, x)$ for one point $x = (0, 0, \dots, 0)^\top \in \mathbb{R}^d$ as the deep BSDE method is only designed for finding solution at a single point while our method can in fact give solution in a region at once where the $X_0 = x$ is sampled. The deep BSDE is implemented with the code publicly available from the website² to solve HJB-2 introduced in subsection 4.4, where the infimum Hamiltonian $\inf_u H$ is computed by its explicit form. At each time step, the deep BSDE employs a fully connected neural network with two hidden layers, each containing W_h units, to approximate the policy function. Other hyperparameters align with those used in example (13) of [21]. For the SOC-MartNet, Algorithm 3.1 is applied to HJB-2 without using the explicit $\inf_u H$. Both networks u_α and v_θ in SOC-MartNet are structured with four hidden layers, each comprising W_h units. The values of W_h used are reported in the numerical results. Both methods are implemented on a single GPU (NVIDIA A100-SXM4-80GB) with a needed number I of iterations to reach a comparable accuracy, with $I = 1000$ iterations for the SOC-MartNet and $I = 2000$ for the deep BSDE. Table 1 reports the errors and running times.

As shown in Table 1, although SOC-MartNet does not rely on the explicit $\inf_u H$, it still achieves accuracy, using shorter running times, comparable to the deep BSDE and its efficiency stems from the parallel nature in the computation of the loss functions in (3.30) and (3.31) across time and space.

We further highlight that the efficiency of our method can be significantly enhanced through the use of multiple GPU parallel computing. Specifically, we apply

²<https://github.com/frankhan91/DeepBSDE>

Table 1: The REs and running times (RTs) of SOC-MartNet (Algorithm 3.1) and deep BSDE for solving HJB-2 introduced in subsection 4.4. The number of iteration steps is $I = 1000$ for SOC-MartNet and $I = 2000$ for deep BSDE.

Network width	d	RE		SD		RT	
		Deep BSDE	SOC-MartNet	Deep BSDE	SOC-MartNet	Deep BSDE	SOC-MartNet
$W_h = 256$	100	3.23E-03	1.24E-03	8.90E-04	2.43E-03	73	48
	300	1.18E-03	1.14E-03	8.19E-04	1.20E-03	90	53
	500	1.05E-03	2.89E-03	5.71E-04	1.22E-03	116	58
	800	2.54E-03	4.35E-03	1.90E-03	1.41E-03	145	73
	1000	1.86E-03	5.83E-03	2.08E-03	2.57E-03	170	118
$W_h = d + 10$	100	2.86E-03	2.94E-03	1.09E-03	1.67E-03	53	20
	300	3.27E-04	8.99E-04	1.27E-04	1.02E-03	103	51
	500	6.41E-04	6.92E-04	3.58E-04	4.99E-04	184	103
	800	1.28E-03	4.00E-03	1.14E-03	3.78E-03	386	255
	1000	3.77E-03	1.11E-03	5.87E-03	4.26E-04	615	360

Table 2: The running times (unit: second) of SOC-MartNet (Algorithm 3.1) for solving HJB-3 introduced in subsection 4.4. The algorithm is accelerated by DDP on multiple GPUs. The number of iteration steps and the network widths are set to $I = 6000$ and $W_h = d + 10$, respectively.

GPUs	$d = 100$	$d = 500$	$d = 800$	$d = 1000$	$d = 2000$
$1 \times \text{A100}$	153	775	1350	1909	5032
$2 \times \text{A100}$	151	430	721	1001	2582
$4 \times \text{A100}$	142	233	393	536	1387
$8 \times \text{A100}$	148	153	231	302	773

the SOC-MartNet (Algorithm 3.1) to HJB-3, and record the running times under different numbers of GPUs used by DDP. The relevant results are presented in Table 2. Notably, the SOC-MartNet can be accelerated significantly by the DDP for the problem with dimensionality $d \geq 500$.

5. Conclusions and future work. In this paper, we propose a martingale-based DNN method for stochastic optimal controls, SOC-MartNet, based on the original DeepMartNet [5, 6] combined with adversarial learning. A Hamiltonian process and a cost process are introduced using a control network and a value network. A loss function for the networks' training is used to ensure the minimum principle for the optimal feedback control as well as the fulfillment of the HJB equation by the value function, and the latter is implemented through a martingale formulation and a training that drives the value function network to satisfy its martingale properties at convergence. In SOC-MartNet, the martingale property of the cost process is however enforced by an adversarial learning, whose loss function is built upon the projection property of conditional expectations. Numerical results show that the proposed SOC-MartNet is effective and efficient for solving HJB-type equations with dimension up to 10,000 in a small number of stochastic gradient method iterations (less than 6000) for the training, and particularly, for SOCPs where the $\inf H$ has no explicit expressions.

For future work, we will carry out theoretical analysis to study the convergence of the proposed SOC-MartNet and provide some mathematical justification of the

observed computational performance of the method.

Acknowledgments. The authors thank Alain Bensoussan for helpful discussion on the HJB equation and stochastic optimal controls.

REFERENCES

- [1] A. BACHOUCH, C. HURÉ, N. LANGRENÉ, AND H. PHAM, *Deep neural networks algorithms for stochastic control problems on finite horizon: numerical applications*, Methodol. Comput. Appl. Probab., 24 (2022), pp. 143–178.
- [2] G. BARLES AND E. R. JAKOBSEN, *On the convergence rate of approximation schemes for Hamilton-Jacobi-Bellman equations*, M2AN Math. Model. Numer. Anal., 36 (2002), pp. 33–54.
- [3] R. BELLMAN, *Dynamic programming*, Princeton University Press, Princeton, NJ, 1957.
- [4] S. CACACE, E. CRISTIANI, M. FALCONE, AND A. PICARELLI, *A patchy dynamic programming scheme for a class of Hamilton-Jacobi-Bellman equations*, SIAM J. Sci. Comput., 34 (2012), pp. A2625–A2649.
- [5] W. CAI, *DeepMartNet – a martingale based deep neural network learning algorithm for eigenvalue/BVP problems and optimal stochastic controls*, 2023, [https://arxiv.org/abs/arXiv:2307.11942\[math.NA\]](https://arxiv.org/abs/arXiv:2307.11942[math.NA]).
- [6] W. CAI, A. HE, AND D. MARGOLIS, *DeepMartNet – a martingale based deep neural network learning method for Dirichlet BVP and eigenvalue problems of elliptic pdes*, 2023, [https://arxiv.org/abs/arXiv:2311.09456\[math.NA\]](https://arxiv.org/abs/arXiv:2311.09456[math.NA]).
- [7] R. CARMONA, *Lectures on BSDEs, stochastic control, and stochastic differential games with financial applications*, vol. 1 of Financial Mathematics, Society for Industrial and Applied Mathematics (SIAM), Philadelphia, PA, 2016.
- [8] M. G. CRANDALL, H. ISHII, AND P.-L. LIONS, *User’s guide to viscosity solutions of second order partial differential equations*, Bull. Amer. Math. Soc. (N.S.), 27 (1992), pp. 1–67.
- [9] J. DARBON, P. M. DOWER, AND T. MENG, *Neural network architectures using min-plus algebra for solving certain high-dimensional optimal control problems and hamilton-jacobi pdes*, Mathematics of Control, Signals, and Systems, 35 (2023), pp. 1–44.
- [10] J. DARBON, G. P. LANGLOIS, AND T. MENG, *Overcoming the curse of dimensionality for some Hamilton-Jacobi partial differential equations via neural network architectures*, Res. Math. Sci., 7 (2020), pp. Paper No. 20, 50.
- [11] J. DARBON AND T. MENG, *On some neural network architectures that can represent viscosity solutions of certain high dimensional Hamilton-Jacobi partial differential equations*, J. Comput. Phys., 425 (2021), pp. Paper No. 109907, 16.
- [12] S. DOLGOV, D. KALISE, AND K. K. KUNISCH, *Tensor decomposition methods for high-dimensional Hamilton-Jacobi-Bellman equations*, SIAM J. Sci. Comput., 43 (2021), pp. A1625–A1650.
- [13] W. E, J. HAN, AND A. JENTZEN, *Deep learning-based numerical methods for high-dimensional parabolic partial differential equations and backward stochastic differential equations*, Commun. Math. Stat., 5 (2017), pp. 349–380.
- [14] W. H. FLEMING AND R. W. RISHEL, *Deterministic and stochastic optimal control*, vol. No. 1 of Applications of Mathematics, Springer-Verlag, Berlin-New York, 1975.
- [15] Y. FU, W. ZHAO, AND T. ZHOU, *Highly accurate numerical schemes for stochastic optimal control via FBSDEs*, Numer. Math. Theory Methods Appl., 13 (2020), pp. 296–319.
- [16] Z. GAO, L. YAN, AND T. ZHOU, *Failure-informed adaptive sampling for PINNs*, SIAM J. Sci. Comput., 45 (2023), pp. A1971–A1994.
- [17] M. GERMAIN, H. PHAM, AND X. WARIN, *Approximation error analysis of some deep backward schemes for nonlinear PDEs*, SIAM J. Sci. Comput., 44 (2022), pp. A28–A56.
- [18] B. GONG, W. LIU, T. TANG, W. ZHAO, AND T. ZHOU, *An efficient gradient projection method for stochastic optimal control problems*, SIAM J. Numer. Anal., 55 (2017), pp. 2982–3005.
- [19] L. GUO, H. WU, X. YU, AND T. ZHOU, *Monte Carlo fPINNs: deep learning method for forward and inverse problems involving high dimensional fractional partial differential equations*, Comput. Methods Appl. Mech. Engrg., 400 (2022), pp. Paper No. 115523, 17.
- [20] J. HAN AND W. E, *Deep learning approximation for stochastic control problems*, Deep Reinforcement Learning Workshop, NIPS, (2016), [https://arxiv.org/abs/arXiv:1611.07422\[cs.LG\]](https://arxiv.org/abs/arXiv:1611.07422[cs.LG]).
- [21] J. HAN, A. JENTZEN, AND W. E, *Solving high-dimensional partial differential equations using deep learning*, Proceedings of the National Academy of Sciences, 115 (2018), pp. 8505–8510.

- [22] J. HAN AND J. LONG, *Convergence of the deep BSDE method for coupled FBSDEs*, Probab. Uncertain. Quant. Risk, 5 (2020), pp. Paper No. 5, 33, <https://doi.org/10.1186/s41546-020-00047-w>, <https://doi.org/10.1186/s41546-020-00047-w>.
- [23] D. HE, S. LI, W. SHI, X. GAO, J. ZHANG, J. BIAN, L. WANG, AND T.-Y. LIU, *Learning physics-informed neural networks without stacked back-propagation*, in Proceedings of The 26th International Conference on Artificial Intelligence and Statistics, F. Ruiz, J. Dy, and J.-W. van de Meent, eds., vol. 206 of Proceedings of Machine Learning Research, PMLR, 25–27 Apr 2023, pp. 3034–3047.
- [24] Z. HU, K. SHUKLA, G. E. KARNIADAKIS, AND K. KAWAGUCHI, *Tackling the curse of dimensionality with physics-informed neural networks*, Neural Networks, 176 (2024), p. 106369.
- [25] C. HURÉ, H. PHAM, A. BACHOUCH, AND N. LANGRENÉ, *Deep neural networks algorithms for stochastic control problems on finite horizon: convergence analysis*, SIAM J. Numer. Anal., 59 (2021), pp. 525–557.
- [26] C. HURÉ, H. PHAM, AND X. WARIN, *Deep backward schemes for high-dimensional nonlinear PDEs*, Math. Comp., 89 (2020), pp. 1547–1579.
- [27] H. ISHII, *On uniqueness and existence of viscosity solutions of fully nonlinear second-order elliptic PDEs*, Comm. Pure Appl. Math., 42 (1989), pp. 15–45.
- [28] S. JI, S. PENG, Y. PENG, AND X. ZHANG, *Solving stochastic optimal control problem via stochastic maximum principle with deep learning method*, J. Sci. Comput., 93 (2022), pp. Paper No. 30, 28.
- [29] D. KALISE AND K. KUNISCH, *Polynomial approximation of high-dimensional Hamilton-Jacobi-Bellman equations and applications to feedback control of semilinear parabolic PDEs*, SIAM J. Sci. Comput., 40 (2018), pp. A629–A652.
- [30] W. KANG AND L. C. WILCOX, *Mitigating the curse of dimensionality: sparse grid characteristics method for optimal feedback control and HJB equations*, Comput. Optim. Appl., 68 (2017), pp. 289–315.
- [31] I. KHARROUBI, N. LANGRENÉ, AND H. PHAM, *A numerical algorithm for fully nonlinear HJB equations: an approach by control randomization*, Monte Carlo Methods Appl., 20 (2014), pp. 145–165.
- [32] I. KHARROUBI, N. LANGRENÉ, AND H. PHAM, *Discrete time approximation of fully nonlinear HJB equations via BSDEs with nonpositive jumps*, Ann. Appl. Probab., 25 (2015), pp. 2301–2338.
- [33] I. KHARROUBI AND H. PHAM, *Feynman-Kac representation for Hamilton-Jacobi-Bellman IPDE*, Ann. Probab., 43 (2015), pp. 1823–1865.
- [34] A. KLENKE, *Probability Theory*, Springer Cham, third ed., 2020.
- [35] P. E. KLOEDEN AND E. PLATEN, *Numerical solution of stochastic differential equations*, vol. 23 of Applications of Mathematics (New York), Springer-Verlag, Berlin, 1992.
- [36] N. V. KRYLOV, *Nonlinear elliptic and parabolic equations of the second order*, vol. 7 of Mathematics and its Applications (Soviet Series), D. Reidel Publishing Co., Dordrecht, 1987. Translated from the Russian by P. L. Buzytsky [P. L. Buzytskiĭ].
- [37] H. J. KUSHNER AND P. DUPUIS, *Numerical methods for stochastic control problems in continuous time*, vol. 24 of Applications of Mathematics (New York), Springer-Verlag, New York, second ed., 2001. Stochastic Modelling and Applied Probability.
- [38] X. LI, D. VERMA, AND L. RUTHOTTO, *A neural network approach for stochastic optimal control*, SIAM J. Sci. Comput., 46 (2024), pp. C535–C556.
- [39] P.-L. LIONS, *Generalized solutions of Hamilton-Jacobi equations*, vol. 69 of Research Notes in Mathematics, Pitman (Advanced Publishing Program), Boston, Mass.-London, 1982.
- [40] T. NAKAMURA-ZIMMERER, Q. GONG, AND W. KANG, *Adaptive deep learning for high-dimensional Hamilton-Jacobi-Bellman equations*, SIAM J. Sci. Comput., 43 (2021), pp. A1221–A1247.
- [41] S. OSHER AND C. SHU, *High-order essentially nonoscillatory schemes for hamilton-jacobi equations*, SIAM Journal on numerical analysis, 4 (1991), pp. 907–922.
- [42] H. PHAM, *Continuous-time stochastic control and optimization with financial applications*, vol. 61 of Stochastic Modelling and Applied Probability, Springer-Verlag, Berlin, 2009.
- [43] M. RAISSI, *Forward-backward stochastic neural networks: Deep learning of high-dimensional partial differential equations*, 2018, [https://arxiv.org/abs/arXiv:1804.07010\[stat.ML\]](https://arxiv.org/abs/arXiv:1804.07010[stat.ML]).
- [44] M. RAISSI, P. PERDIKARIS, AND G. E. KARNIADAKIS, *Physics-informed neural networks: a deep learning framework for solving forward and inverse problems involving nonlinear partial differential equations*, J. Comput. Phys., 378 (2019), pp. 686–707.
- [45] S. RICHARDSON AND S. WANG, *Numerical solution of Hamilton-Jacobi-Bellman equations by an exponentially fitted finite volume method*, Optimization, 55 (2006), pp. 121–140.
- [46] R. J. E. SAMUEL N. COHEN, *Stochastic Calculus and Applications*, Birkhäuser New York, NY,

- 2015.
- [47] I. SMEARS AND E. SÜLI, *Discontinuous Galerkin finite element approximation of Hamilton-Jacobi-Bellman equations with Cordes coefficients*, SIAM J. Numer. Anal., 52 (2014), pp. 993–1016.
 - [48] C. WANG, S. LI, D. HE, AND L. WANG, *Is l^2 physics informed loss always suitable for training physics informed neural network?*, in Advances in Neural Information Processing Systems, A. H. Oh, A. Agarwal, D. Belgrave, and K. Cho, eds., 2022.
 - [49] J. YONG AND X. Y. ZHOU, *Stochastic controls*, vol. 43 of Applications of Mathematics (New York), Springer-Verlag, New York, 1999. Hamiltonian systems and HJB equations.
 - [50] Y. ZANG, G. BAO, X. YE, AND H. ZHOU, *Weak adversarial networks for high-dimensional partial differential equations*, J. Comput. Phys., 411 (2020), pp. 109409, 14.
 - [51] W. ZHANG AND W. CAI, *FBSDE based neural network algorithms for high-dimensional quasi-linear parabolic PDEs*, J. Comput. Phys., 470 (2022), pp. Paper No. 111557, 14.
 - [52] W. ZHAO, T. ZHOU, AND T. KONG, *High order numerical schemes for second-order FBSDEs with applications to stochastic optimal control*, Commun. Comput. Phys., 21 (2017), pp. 808–834.
 - [53] M. ZHOU, J. HAN, AND J. LU, *Actor-critic method for high dimensional static Hamilton-Jacobi-Bellman partial differential equations based on neural networks*, SIAM J. Sci. Comput., 43 (2021), pp. A4043–A4066.